Electronic Supplementary Material (ESI) for Materials Horizons.

Supplementary Document to "Magnetoelectricity Beyond Saturation" by S. Newacheck and G. Youssef

Nomenclature

C_{ij}	Elastic coefficients
ρ	Mass density
ε_{ij}	Strain
σ_{ij}	Stress
H_i	Magnetic field
B_i	Magnetic flux
χ_i	Magnetic susceptibility
q_{ij}	Piezomagnetic coefficients
E_i	Electric field
e_{ij}	Piezoelectric coefficients

1. Sample and experimental details

The multiferroic composite structure was fabricated by bonding a radially poled PZT cylinder to an inner Terfenol-D cylinder using a silver conductive epoxy as discussed the main paper. The PZT cylinder had an outer diameter of 30mm, inner diameter of 25mm, and height of 5mm, whereas the Terfenol-D cylinder had an outer diameter, inner diameter, and height of 25mm, 20mm, and 5mm, respectively. The basic physical and mechanical properties for PZT and Terfenol-D are listed in Supplementary Table 1. While the dimensions of the test structure was obviously on the macroscale, similar configuration can be realized on the micro and nano scales using physical and chemical vapor deposition processes such as magnetron sputtering and atomic layer deposition, respectively. Notably, different piezomagnetic and magnetostrictive materials were previously deposited on numerous substrates using these deposition techniques (see [1], [2]).

Supplementary Table 1. Material Properties of PZT and Terfenol-D

Material	Property	Value	Unit
PZT-5A	ρ	7500	[kg m^{-3}]
	C_{11}	99.201	[GPa]
	C_{13}	50.778	[GPa]
	C_{33}	86.856	[GPa]
	e_{13}	-7.209	[N C^{-1}]
	e_{33}	15.118	[N C^{-1}]
	ε_{33}	1.5 E-8	[C^2 N^{-1} m^{-2}]
Terfenol-D	ρ	9200	[kg m^{-3}]
	C_{11}	8.451	[GPa]
	C_{13}	3.91	[GPa]
	C_{33}	28.3	[GPa]
	q_{13}	-5.75	[N A^{-1} m^{-1}]
	q_{33}	270.1	[N A^{-1} m^{-1}]

The magnetoelectric coupling coefficient at the center of the fabricated composite sample was characterized in response to actuation of the outer PZT cylinder at 20 kV/m electric field at different frequencies (listed in the main paper) and an increasing bias magnetic field (range provided on the abscissa of Figure 1 in the paper). The AC electric field was radially applied using a function generator (Agilent 33210 A) and a high voltage amplifier (TREK PZD700A). The bias magnetic field was applied diametrically using an electromagnet (GMW 3470). The resulting CME was measured using a lock-in amplifier (SRS 830) connected to the centrally-located search coil. The data was collected using a built in-house data acquisition system.

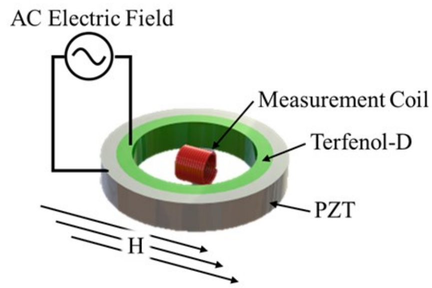

Supplementary Figure 1. Schematic of the experimental setup showing the composite cylinder, the centrally-located search coil to measure the response, and applied boundary conditions.

2. Magneto-mechanical properties of ferromagnetic materials

The linear constitutive relationship of magnetostrictive materials used to solve for strain-mediated magnetoelectric composite systems is given by SEQ 1.

$$B = \chi H + q\varepsilon \qquad \text{(SEQ 1a)}$$
$$\varepsilon = S\sigma + qH \qquad \text{(SEQ 1b)}$$

Where, S is the mechanical compliance defined as the inverse of the elasticity coefficient matrix. Although the material properties are generally reported as nominal values, as seen in Supplementary Table 1, these properties are known to be dependent on the bias magnetic field as demonstrated schematically in Supplementary Figure 2. Supplementary Figure 2A shows the B-H relationship (the first term of SEQ 1a) where the initial slope is the magnetic susceptibility. Conversely, the magnetostrictive strain in response to the magnetic field (the second part of SEQ1b) is shown in Supplementary Figure 2B, where the slope is the piezomagnetic coefficient defining the magneto-mechanical response. The maximum magnetostrictive strain typically reaches from 800 to 1200 ppm when magnetic saturation is reached, which reported being 1000 Oe for Terfenol-D. Due to the importance of the piezomagnetic response for ME composites, Supplementary Figure 2C schematically plots the piezomagnetic coefficient as a function of the magnetic field. The piezomagnetic curve in Supplementary Figure 2C can be thought of as the derivative of the magnetostrictive curve in Supplementary Figure 1B. For reference, the peak piezomagnetic coefficient is referred to as the piezomagnetic region, which is around 375-500 Oe for Terfenol-D. Finally, Supplementary Figure 2D shows the stiffness with respect to the magnetic field applied, where the change is due to the delta-E effect. The stiffness of Terfenol-D ranges from 18 to 90 GPa depending on the magnetic field applied [3].

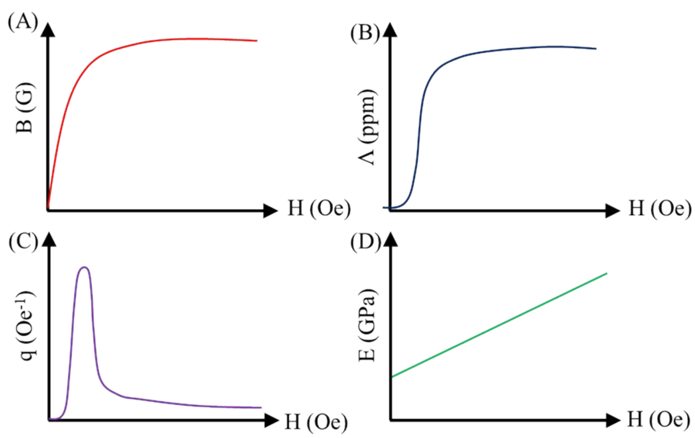

Supplementary Figure 2. Schematic representations of the properties of ferromagnetic materials in response to a magnetic field, A) magnetic flux, B) magnetostriction, C) piezomagnetic, D) Young's Modulus.

3. Evidence of non-uniform magneto-mechanical response

As discussed in the main article, the primary mediator between the electric and magnetic energies is the mechanical strain. In the case of the converse magnetoelectric coupling paradigm, the application of a bias magnetic field, to activate Terfenol-D magnetic response, and the AC electrical field to transduce the strain results in emanation of the magnetic field, which is noted to be non-uniform. Therefore, probing the strain around the circumference gives a visual indication of the nonuniformity of the state of magnetization around the cylinder. In a previous report [4], strain gauges were attached to a lone Terfenol-D cylinder with identical dimensions to the component used for the composite structure. The strain gauges were placed to measure the radial and circumferential magnetostrictive response at various locations around the Terfenol-D cylinder as a function of the bias magnetic field. The results of radial and circumferential strain are plotted in Supplementary Figure 4A and 4C, respectively, whereas the locations of the measurements are in the inset of each subfigure. The magnetostriction at the zenith locations (90° and 270°) are quickly reaching the magnetic saturation resembling behaviors similar to the schematic illustration in Supplementary Figure 2B. These locations are the earlier contributors to the overall CME observed at the center of the composite cylinder, referred to as the climax of the response in the accompanying paper. However, the magnetization at the poles (0° and 180°) show little to no magnetization even beyond the saturation field of 2000 Oe. Additionally, the locations between the poles and zenith (45°) only exhibit a moderate magnetization. The evidence of Supplementary Figure 4 supports the delineated hypothesis about the underlying mechanism leading to the reported magnetoelectricity beyond saturation; a unique feature of the cylindrical structure in multiferroic composites.

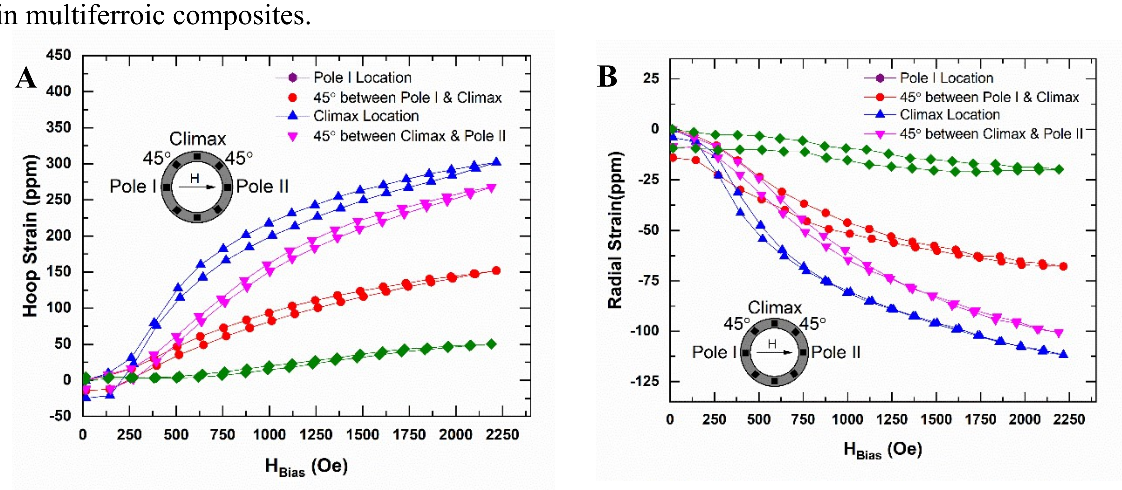

Supplementary Figure 4. The A) hoop and B) radial magnetostrictive strains with respect to the bias magnetic field (reproduced from [4]).

4. Experimental evidence of the cylindrical structure to the CME beyond saturation

The main hypothesis leading to the reported magnetoelectric response at higher magnetic fields is based on the delayed magnetic saturation of different regions around the circumference of the cylinder. Hence, contrasting the CME response measured locally on the cylinder with the CME measured remotely at the center provides the remaining experimental evidence supporting the validity of the stated hypothesis. Supplementary Figure 5A shows a schematic of the experimental setup used to measure the localized CME on the cylinder, which was identical to the one used to generate the data reported in the main manuscript (see Section 1 above). In Supplementary Figure 5B, the localized and remote CME response at 34 kHz in response to an extended range of bias magnetic fields [5]. The results show that the localized CME reaches the maximum at a low magnetic field due to the saturation of the Terfenol-D under the search coil, where further increase in the magnetic field had no effect on the response. However, the CME measured using the centrally-located search coil continues to climb to reach a maxim at higher magnetic field due to the participation of adjacent regions on the cylinder as the magnetic field is increased. That is, as an additional regions on the cylinder reach magnetic saturation and emanate field that is sensible at the center, the CME value increases signifying the magnetoelectricity beyond saturation.

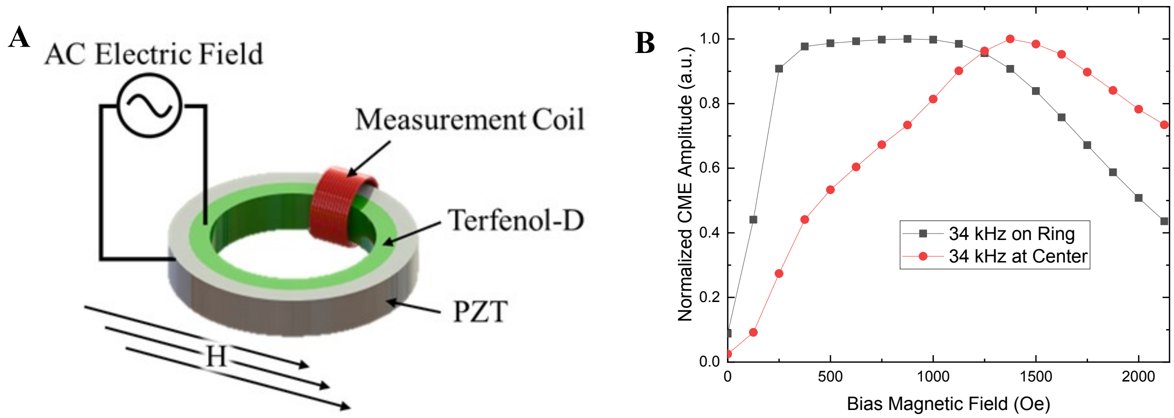

Supplementary Figure 5. A) Schematic of the on ring CME setup, and B) the CME as a function of the bias magnetic field.

References

[1] M. Klaui, C. A. F. Vaz, L. Lopez-Diaz, and J. A. C. Bland, “Vortex formation in narrow ferromagnetic rings,” *J. Phys. Condens. Matter*, vol. 15, no. 21, p. R985, 2003.

[2] C. L. Jia *et al.*, “Unit-cell scale mapping of ferroelectricity and tetragonality in epitaxial ultrathin ferroelectric films,” *Nat. Mater.*, vol. 6, no. 1, pp. 64–69, 2007.

[3] R. Kellogg and A. Flatau, “Experimental Investigation of Terfenol-D ’ s Elastic Modulus,” *J. Intell. Mater. Syst. Struct.*, vol. 19, no. May, pp. 583–595, 2008.

[4] G. Youssef, S. Newacheck, and M. Lopez, “Mapping magnetoelastic response of terfenol-D ring structure,” *Appl. Phys. Lett.*, vol. 110, no. 19, p. 192408, 2017.

[5] G. Youssef, M. Lopez, and S. Newacheck, “On the effect of polarization direction on the converse magnetoelectric response of multiferroic composite rings,” *Smart Mater. Struct.*, vol. 26, no. 3, p. 037003, 2017.